Materials Science and Engineering A 402 (2005) 92–97

www.elsevier.com/locate/msea

Effect of alloying elements and processing factors on the microstructure and hardness of sintered and induction-hardened Fe–C–Cu alloys

Wen-Fung Wang *

Department of Mechanical Engineering, Southern Taiwan University of Technology, Tainan, Taiwan

Accepted 5 April 2005

Abstract

The SC 100.26 iron powder and the PASC 60 powder (with a P content of 0.6 wt%) were mixed with graphite and copper powders. The blended powder mixtures were compacted, sintered and the P-containing sintered alloys were then induction-hardened. Experimental results show that the microstructure of sintered Fe–C–Cu alloys varies with the copper content. The proeutectoid ferrite becomes refined and decreases in volume when the copper content is increased. The ferritic phase is markedly hardened by the dissolved copper. The P-containing specimens exhibit marked volume expansion following sintering. The volume dilation increases with increasing compacting pressure. The hardness of sintered Fe–C–Cu–P alloys increases with increasing compacting pressure and carbon content. Further strengthening is resulted from the strong solution hardening effect of phosphorus in iron. Hardness variation of sintered alloys, with the carbon content, is dependent on the compacting pressure. Following induction hardening the surface hardness also increases with increasing carbon content and compacting pressure, but by a different mode from that in the as-sintered state. This is promoted by the phosphorus addition.

Keywords: Fe–C–Cu sintered alloys; Phosphorus; Induction hardening; Hardness

1. Introduction

Mixtures of elemental iron and graphite powders are commonly used for P/M application. A small amount of copper powder is always added to further strengthen the sintered alloys owing to its relative ease of dissolving and diffusing in the iron matrix upon sintering. Extensive investigations on the sintering properties of Fe–Cu and Fe–C–Cu alloys made from elemental powders are well reported [1–12]. However, few studies have been conducted to investigate the effect of copper content on the microstructure of sintered carbon steels.

In the past two decades, the positive role of phosphorus in ferrous powder metallurgy has been also well recognized [13,14]. Phosphorus is usually considered a contaminating element in conventional steels, because of its tendency for segregation at grain boundaries causing brittleness and its low diffusion in iron. Nevertheless, phosphorus acts as a strong enhancer of the sintering process, enabling the time or temperature to be reduced. Among the substitutive alloying elements in iron, phosphorus has the strongest solid solution hardening effect on ferrite. The physical and mechanical characteristics of P/M Fe–P, Fe–C–P and Fe–C–Cu–P alloys have been studied by many authors [15–21].

Fe–C–P or Fe–C–Cu–P alloys are therefore of great interest for structural applications. They combine the favorable morphology of porosity and the good mechanical properties. To further increase the strength and hardness, heat treatments of quenching and tempering are often performed on sintered structural parts. However, the results for the P-containing sintered steels are not encouraging, since during heat treatment these alloys present the phenomenon of phosphorus grain boundary segregation (PGBS). The PGBS results in brittleness, which is unacceptable for any structural application [23]. These alloys, therefore, appear to be suitable only for application in the as-sintered state. The P-containing sintered iron alloys have been subjected to both plasma nitriding (carried out at 650 °C for 24 h) and gaseous case hardening (carried out at 860 °C for 60 min). During high temperature treatment segregation of phosphorus occurs. In the surface

* Tel.: +886 6 2281 663; fax: +886 6 268 5257.
E-mail address: wfwang@mail.stut.edu.tw.

0921-5093/$ – see front matter © 2005 Elsevier B.V. All rights reserved.
doi:10.1016/j.msea.2005.04.016

layer fracture occurs through cleavage [22]. Therefore, the furnace hardening treatment and surface hardening, such as nitriding and gaseous case hardening are not suitable to be performed on the P-containing sintered iron alloys. The present study is devoted to study the effect of copper content on the morphology and microstructure of the ferritic phase of sintered hypereutectoid Fe–C–Cu alloys; to investigate the effect of compacting pressure, carbon content and phosphorus addition on the bulk hardness of the sintered Fe–C–Cu–P steels and their surface hardness after induction hardening.

2. Experimental

Iron based sintered alloys were obtained from elementary mixtures of three types of powders: ferrophosphorus with a composition of Fe–0.6 wt%P, known commercially as PASC 60, 2 wt% atomized copper powder (−325 mesh) and natural graphite powders. The physical properties of iron powders are shown in Table 1. Another group of samples used SC 100.26 powder as the matrix, mixed with graphite and copper powders, ranging between 2 and 8 wt%Cu. For both groups of powder mixtures the graphite powder was carefully adjusted so that the sintered alloys contained 0.2, 0.4, 0.6, 0.8 and 1.0 wt%C. The P-containing blended powders were compacted into specimens of 25 mm × 25 mm × 7 mm with a pressure of 400, 500, 600 and 700 MPa. The non-P powder mixtures were consolidated only with a pressure of 500 MPa. The green compacts were then sintered at 1140 °C for 40 min in the cracked ammonia. The dew point of furnace atmosphere is −30 °C, and the cooling rate of sintering furnace is 8 °C/min. The sintering practice was performed in an industrial plant. One square side (25 mm × 25 mm) of the P-containing sintered alloys was induction-heated with a frequency of 400 kHz for 2 s, and then quenched into water. The hardened depth was about 2 mm.

The green and sintered densities were calculated from the volume and weight measurement of specimens before and after sintering. The micro-Vickers hardness testing was carried out on the proeutectoid ferrite and pearlite of sintered Fe–C–Cu alloys. Rockwell B-scale and C-scale hardness measurements were performed on sintered and induction-hardened Fe–C–Cu–P alloys, respectively. The average value of six readings was recorded for each hardness point. Metallography of the sintered alloys was performed with an optical microscope.

3. Results and discussion

3.1. Effect of the copper content on the microstructure of sintered Fe–C–Cu alloys

Metallographic observation of the sintered Fe–0.4 wt%C, Fe–0.4 wt%C–2 wt%Cu, Fe–0.4 wt%C–8 wt%Cu, Fe–0.6 wt%C, Fe–0.6 wt%C–2 wt%Cu and Fe–0.6 wt%C–8 wt%Cu alloys are shown in Fig. 1. It is found that the microstructure of sintered hypoeutectic Fe–C–Cu alloys varies with copper content, the morphology of the proeutectoid ferrite alters remarkably. Carefully examining from Fig. 1a–c and d–f, it can be seen in both groups of sintered alloys that ferrite becomes refined when the copper content is increased. At the same time, the volume fraction of ferrite slightly decreases with the increasing copper content.

At the sintering temperature, all of the carbon atoms and part of the copper atoms diffuse into the iron powder matrix. A fairly uniform fcc austenite structure is resulted. As sintering is completed, during the subsequent cooling the sintered alloys develop quite different microstructures according to its composition. When sintered alloys are cooled to the two-phase region (ferrite + pearlite), proeutectoid ferrite nucleates at grain boundaries of austenite, then grows along the boundaries and thickens. Copper is an austenite stabilizer. When more copper atoms have dissolved in the austenite grains, nucleation and growth of the ferrite will be suppressed. Therefore, as shown in Fig. 1b and e the volume and thickness of these proeutectoid ferrite decreases with increasing copper content. Further increasing the copper content, as shown in Fig. 1c and f, results in a microstructure with very fine ferrite dispersed along the grain boundaries of the austenite. When the sintered specimens are further cooled below the eutectoid temperature, residual austenite grains subsequently transform into pearlite.

3.2. Effect of the copper content on the microhardness of the ferrite and pearlite phase

To investigate how copper atoms solution-strengthen the constituents of the sintered alloys, the micro-Vickers hardness (HMV) of ferrite and pearlite phase of the Fe–0.4 wt%C, Fe–0.4 wt%C–2 wt%Cu, Fe–0.4 wt%C–4 wt%Cu and Fe–0.4 wt%C–8 wt%Cu alloys were measured. The measured values (average of six readings) are shown in Table 2, and the conclusions are drawn as following:

Table 1
Physical properties of SC100.26 and PASC60 powders

Powder	Particle size distribution (%)				Apparent density (g/cm^3)	Flow (s/50 g)
	−150 μm	−106 μm	−75 μm	−45 μm		
SC100.26	17.1	31.5	33.2	18.2	2.70	32
PASC60	25.3	34.2	24.6	15.9	3.12	25

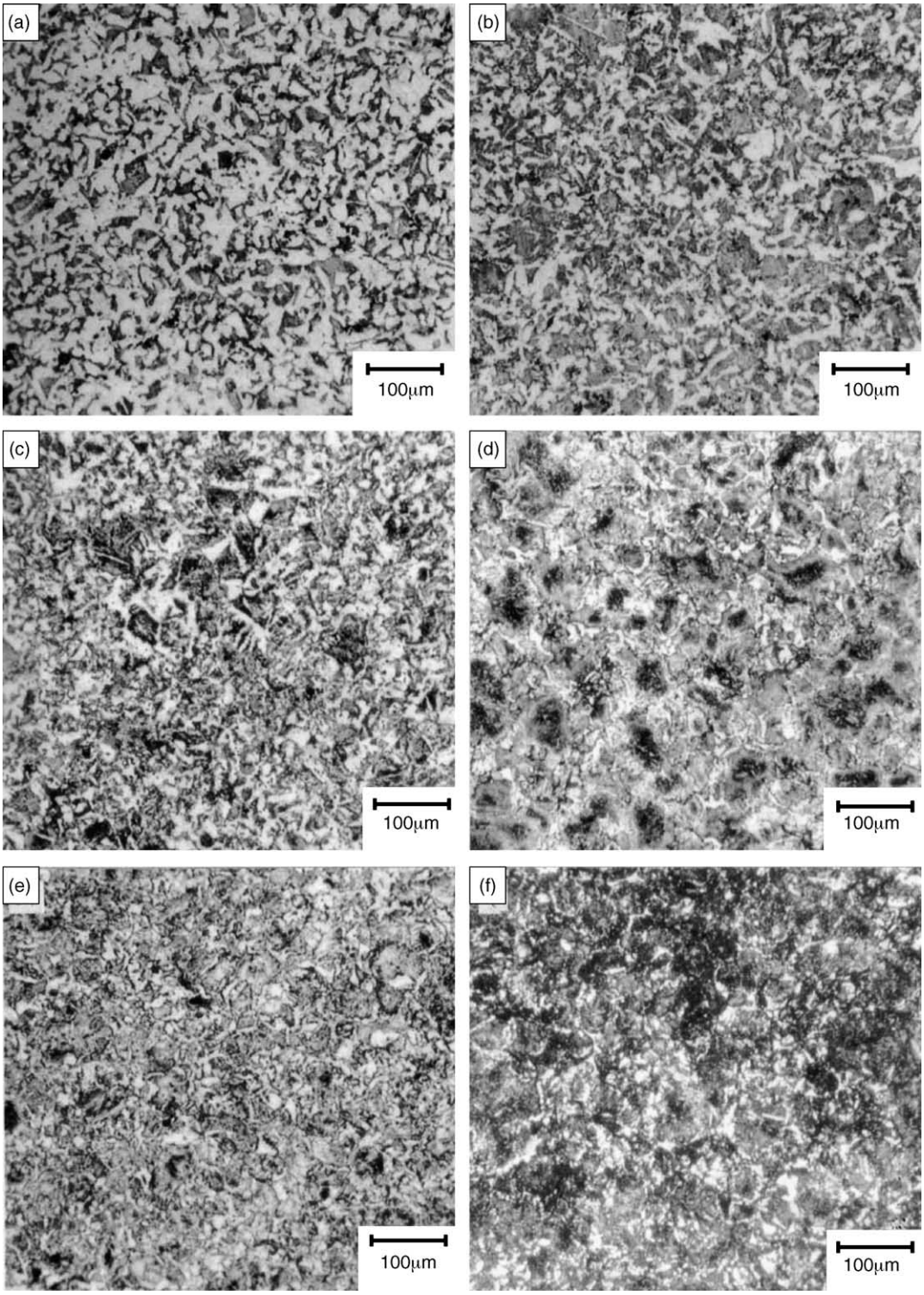

Fig. 1. Micrographs of sintered Fe–C–Cu alloys: (a) Fe–0.4 wt%C, (b) Fe–0.4 wt%C–2 wt%Cu, (c) Fe–0.4 wt%C–8 wt%Cu, (d) Fe–0.6 wt%C, (e) Fe–0.6 wt%C–2 wt%Cu and (f) Fe–0.6 wt%C–8 wt%Cu.

(1) For the Fe–0.4 wt%C alloy, there is a considerable difference between the micro-Vickers hardness values of the ferrite and pearlite, the former is about half of the later.
(2) Addition of 2 wt% of copper markedly hardens the ferrite, the hardness increment is about 90 HMV. The hardness of the pearlite slightly increases; its increment is 23 HMV only. In the pearlite, the hard cementite is predominant, copper strengthening of the laminar eutectoid ferrite can only slightly increase the bulk hardness of this constituent. Consequently, the difference between

Table 2
Variation of the micro-Vickers hardness of ferrite and pearlite phases of sintered Fe–0.4 wt%C–Cu alloys with the copper content (wt%)

	Cu content (wt%)			
	0	2	4	8
Ferrite	105	194	225	244
Pearlite	204	228	256	271

the microhardness of the ferrite and pearlite phase decreases to a value of 34 HMV.

(3) For the Fe–0.4 wt%C–4 wt%Cu and Fe–0.4 wt%C–8 wt%Cu sintered alloys, both of the two constituents are further harden due to more copper dissolution. The hardness difference between the ferrite and pearlite is reduced to a value of 31 and 27 HMV, respectively. The degree of hardness homogeneity is improved.

Comparing the data shown in Table 1, it can be found that the hardness increment of the ferrite resulted from addition of 2 wt% Cu is 89 HMV, while those resulted from addition of 4 and 8 wt% Cu is 120 and 139 HMV, respectively.

3.3. Green and sintered density of the Fe–C–Cu–P alloys

Variation of the green and sintered densities with the compacting pressure and carbon content is shown in Fig. 2. Green density increases with increasing compacting pressure, but the density increment decreases with increasing pressure. Most specimens exhibit volume expansion after sintering. For the P-containing specimens compacted with a pressure of 400, 500 and 600 MPa, the sintered density decreases with increasing carbon content, and then increases. For the group consolidated with a pressure of 700 MPa, the sintered density decreases monotonously with increasing carbon content. For comparison, another batch of Fe–C–Cu (2 wt%) powder mixtures were compacted at a pressure of 500 MPa. The green densities of the P-containing and non-P specimens are nearly the same, but the later ones exhibit better dimensional stability after sintering. The sintered density decreases a little after sintering, and increases slightly with increasing carbon content. The volume change of sintered P-containing specimens is higher than that of the Fe–C–Cu sintered alloys.

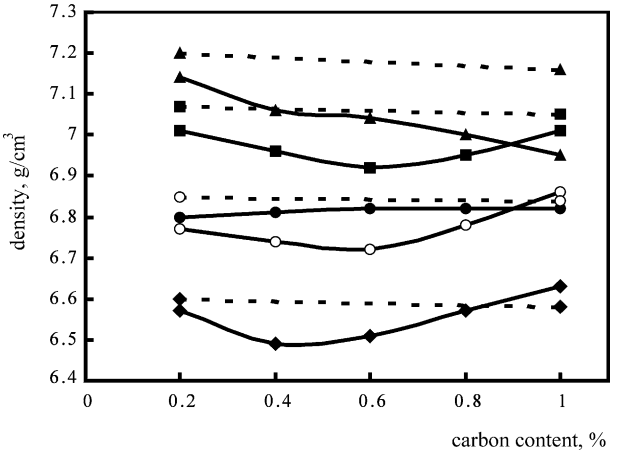

Fig. 2. Variation of green and sintered densities of Fe–C–Cu–P alloys with the compacting pressure and carbon content (dot line, green density; solid line, sintered density (♦) 400 MPa, (◯) 500 MPa, (●) 500 MPa non-P, (■) 600 MPa and (▲) 700 MPa).

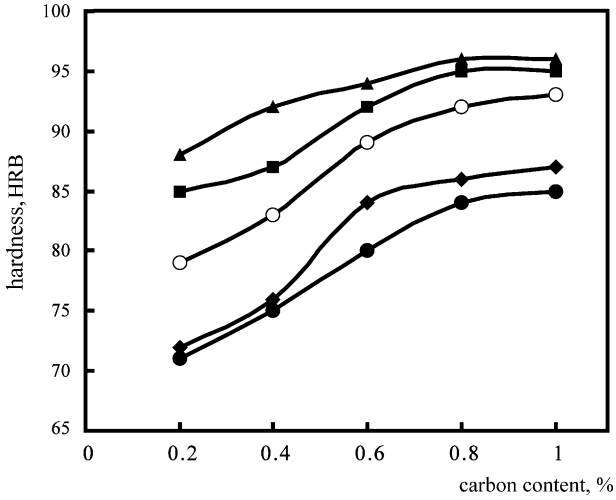

Fig. 3. Variation of the as-sintered hardness of Fe–C–Cu–P alloys with the compacting pressure and carbon content: (♦) 400 MPa, (◯) 500 MPa, (●) 500 MPa non-P, (■) 600 MPa and (▲) 700 MPa.

3.4. Hardness of the sintered Fe–C–Cu–P alloys

Effect of the compacting pressure and carbon content on the hardness of sintered alloys is shown in Fig. 3. The microstructure of sintered carbon steels is a heterogeneous one with different phase content (ferrite and pearlite); therefore, variation of hardness with carbon content is different from that of the sintered density does. The hardness of sintered alloys increases with increasing compacting pressure and carbon content. For the two groups of specimens compacted with a lower pressure of 400 and 500 MPa, hardness increases markedly with increasing carbon content. Increasing of the pearlite volume content profoundly strengthens the sintered alloys. As the compacting pressure applied is further increased to 700 MPa, the hardness of the sintered alloys increases slightly with increasing carbon content. Fig. 2 shows that the sintered density of specimens compacted at a pressure of 700 MPa decreases monotonously with increasing carbon content. This decreasing sintered density partly offsets the strengthening effect resulted from increasing of the pearlite content. The variation mode of the hardness of sintered steels with the carbon content is dependent on the compacting pressure.

Fig. 2 shows that the sintered density of non-P specimens compacted at 500 MPa is higher than those of the P-containing alloys compacted at 400 and 500 MPa. However, the hardness of the non-P alloys is not only lower than that of P-containing ones compacted at the same pressure but also lower than that compacted at 400 MPa. Here reveals the

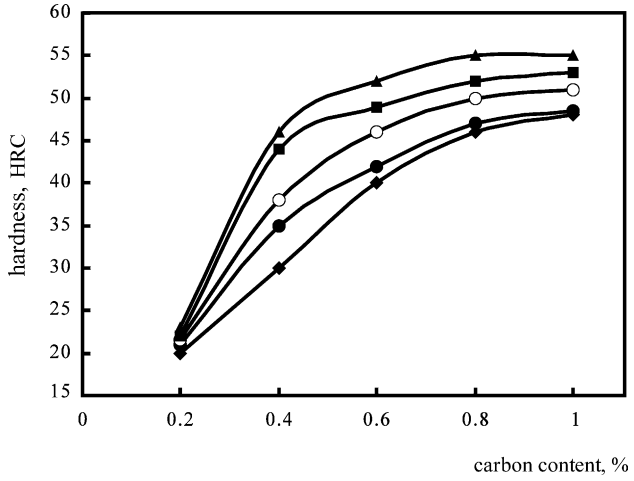

Fig. 4. Variation of the induction-hardened hardness of sintered Fe–C–Cu–P alloys with the compacting pressure and carbon content: (♦) 400 MPa, (◯) 500 MPa, (●) 500 MPa non-P, (■) 600 MPa and (▲) 700 MPa.

strong solution hardening effect of phosphorus in iron; by taking this advantage a lower compacting pressure can be performed to meet the higher hardness requirement by using the P-containing iron powder. Engdahl [19] has pointed out that a heterogeneous distribution of phosphorus in ferrite can positively influence the mechanical properties of sintered materials.

3.5. Induction hardening

Variation of the case hardness of the sintered alloys following induction hardening with the compacting pressure and carbon content is shown in Fig. 4. Hardness of the induction-hardened alloys increases with increasing compacting pressure and carbon content. Hardness increases markedly as the carbon content increases from 0.2 to 0.4 wt%. Pronounced martensite strengthening resulted from increasing carbon content is observed at this stage.

The hardness increment is insignificant as the carbon content is more than 0.8 wt%. Induction austenitizing normally involves rapid heating and requires short holding times, which may lead to variation in carbon content within the austenite grains. Thus, a mixture of high-carbon and low-carbon martensite is formed during quenching. It is the high-carbon martensite which gives rise to higher hardness. This effect decreases in steels whose carbon contents exceed approximately 0.8 wt%, above which the hardness of martensite does not change [24].

For the two groups of specimens compacted at a pressure of 500 MPa, hardness of the P-containing alloys is higher than that of the non-P ones. Phosphorus can afford to further strengthen the induction-hardened sintered alloys. This result is different from Burns et al. [25] and Sykes and Jeffries [26] studies, their experimental data showed that the hardness of furnace hardened and water quenched plain carbon steels and alloy steels is a function only of carbon content. Alloying elements do not affect the hardness of the as-quenched martensite.

For the alloys with a carbon content of 0.2 wt%, the induction-hardened hardness is only slightly affected by the compacting pressure, phosphorus and the as-sintered hardness. The induction-hardened hardness of the non-P alloys compacted at 500 MPa becomes higher than that of the P-containing ones compacted at 400 MPa, though the former is softer than the later in the as-sintered state. During induction heating and quenching higher density can result in better thermal conductivity and subsequently more efficient austenitizing and a higher degree of martensite transformation. The five data curves in Fig. 4 reveal similar shape, which shows that the variation mode of the induction-hardened hardness with the carbon content is not affected by the compacting pressure and phosphorus.

4. Conclusions

The results presented and discussed in this investigation may be summarized in the following points:

1. The morphology of proeutectoid ferrite of the sintered hypoeutectoid Fe–C–Cu alloys is closely related with the copper content. The primary ferrite becomes refined and is progressively solution-strengthened by the increasing copper content.
2. Most Fe–C–Cu–P compacts present volume expansion after sintering, the dimensional stability is inferior to that of the Fe–C–Cu compacts.
3. Hardness of the sintered Fe–C–Cu–P alloys increases with increasing compacting pressure and carbon content, and the phosphorus results in a significant strengthening effect for the as-sintered alloys.
4. Compacting pressure affects the hardness variation mode of sintered Fe–C–Cu–P alloys with increasing carbon content.
5. The case hardness of sintered Fe–C–Cu–P alloys after induction hardening is not a function only of carbon content, and can be further promoted by the phosphorus and the increasing compacting pressure.

References

[1] G. Bockstigal, Metallurgy 3 (1962) 67.
[2] D. Berner, H.E. Exner, G. Petzow, Modern Development in Powder Metallurgy, vol. 6, Princeton, NJ, MPIF, 1974, p. 237.
[3] W.A. Kaysser, W.J. Huppmann, G. Petzow, Powder Metall. 23 (1980) 86.
[4] F.V. Lenel, T. Pencaanha, Powder Metall. 16 (1973) 351.
[5] K. Tabeshhfa, G.A. Chadwick, Powder Metall. 27 (1984) 19.
[6] Y. Wanibe, H. Yokoyama, T. Itoh, Powder Metall. 33 (1990) 65.
[7] Y. Trudel, R. Angers, Modern Development in Powder Metallurgy, vol. 6, Princeton, NJ, MPIF, 1974, 305.
[8] T. Krantz, Int. J. Powder Metall. 25 (1969) 73.
[9] S.J. Jamil, G.A. Chadwick, Powder Metall. 28 (1985) 65.

[10] N. Dautzenberg, H.J. Dorweiler, Powder Metall. Int. 17 (1985) 279.
[11] R.L. Lawcock, T.J. Davie, Powder Metall. 33 (1990) 147.
[12] U. Engstrom, Int. J. Powder Metall. 39 (2003) 29.
[13] F. Lenel, USA Patent No. 2,226,520 (1940).
[14] P. Lindskog, A. Carlsson, Powder Metall. Int. 4 (1972) 39.
[15] P. Lindskog, Powder Metall. 16 (1973) 32.
[16] H. Miura, Y. Tokunaga, Int. J. Powder Metall. Powder Technol. 21 (1985) 269.
[17] M. Hamiuddin, G.S. Upadhyaya, Powder Metall. Int. 14 (1982) 20.
[18] M.A. Siddiqui, M. Hamiuddin, Powder Metall. 29 (1986) 3.
[19] J. Engdahl, Modern Development in Powder Metallurgy, vol. 20, Princeton, NJ, MPIF, 1988, 655.
[20] A. Molinari, G. Straffelini, V. Fontanari, R. Canteri, Powder Metall. 35 (1992) 285.
[21] L.E.G. Cambronero, J.M. Torralba, J.M. Ruiz-Prieto, Powder Metall. Int. 22 (1990) 26.
[22] A. Molinari, G. Straffelini, R. Canteri, Int. J. Powder Metall. 30 (1994) 283.
[23] A. Molinari, G. Straffelini, B. Tesi, Advance Powder Metall. 4 (1992) 13.
[24] S.L. Semiatin, D.E. Stutz, Induction Heat Treatment of Steel, American Society for Metals, Metals Park, OH, 1986.
[25] J.L. Burns, T.L. Moore, R.S. Archer, Trans. ASM 26 (1938) 1.
[26] W.P. Sykes, Z. Jeffries, Trans. ASST 12 (1927) 871.